Using ERI to Apply an Inverse Q* Filter to GPR Data

Eileen Edith Charles*
University of Calgary, Calgary, AB
eileen_e_charles@yahoo.ca

and

Jean-Michel Maillol

Summary

A resistivity model from an inverted electrical resistivity imaging (ERI) survey is used to determine the spatial variation of the Q* parameter along a survey line. The resulting Q* model is used to apply a time and space varying inverse Q* filter to correct for attenuation in the co-located ground penetrating radar (GPR) data. This process is successful in improving the GPR image and helping in the interpretation of a near-surface geophysical study at an archaeological site in Spain.

Introduction

Due to the inherent geophysical ambiguities of an individual survey, a combination of near-surface geophysical techniques is often used to obtain a detailed, three-dimensional characterization of the site (Green et al, 1999). Usually the combination of these techniques is restricted to qualitative interpretation. The mathematical integration of near-surface techniques is an area where development is needed (Meju, 2002).

GPR attenuation is a function of conductivity which is the inverse of resistivity. The Q* parameter was introduced by Turner and Siggens (1994) to characterized GPR attenuation in geological materials. Inverse Q* filtering has been used successfully on GPR data to correct for attenuation (Irving and Knight, 2003).

In this study, a resistivity model from an inverted ERI survey is used to determine the spatial variation of the Q* parameter along a survey line. The resulting Q* model is then used to apply a time and space varying inverse Q* filter to correct for attenuation in the co-located GPR data.

Theory

Absorption is the phenomenon of energy loss due to dielectric losses (conduction and dielectric relaxation). Absorption not only causes a decrease in amplitude as the wave propagates, but also causes distortion of the wavelet. This distortion or broadening of the wavelet is due to higher frequencies being absorbed more than lower frequencies.

The solid curves in Figure 1 show the absorption versus frequency over the entire GPR frequency range for different geological materials. The absorption was calculated from the published fitting parameters (Olhoeft and Capron, 1993). As a GPR signal propagates, the different frequencies are

not absorbed in the same way. However, it is evident that the variation of absorption with frequency is very close to linear over the bandwidth of a GPR antenna (shown in grey).

Since the slope of the absorption versus frequency curve is a straight line, Turner and Siggins (1994) concluded that the change in shape of the wavelet could be described by a single parameter. They defined Q* which is calculated from the slope of the absorption versus frequency graph. This is a generalization of the quality factor commonly used in seismic studies (Kjartansson, 1979).
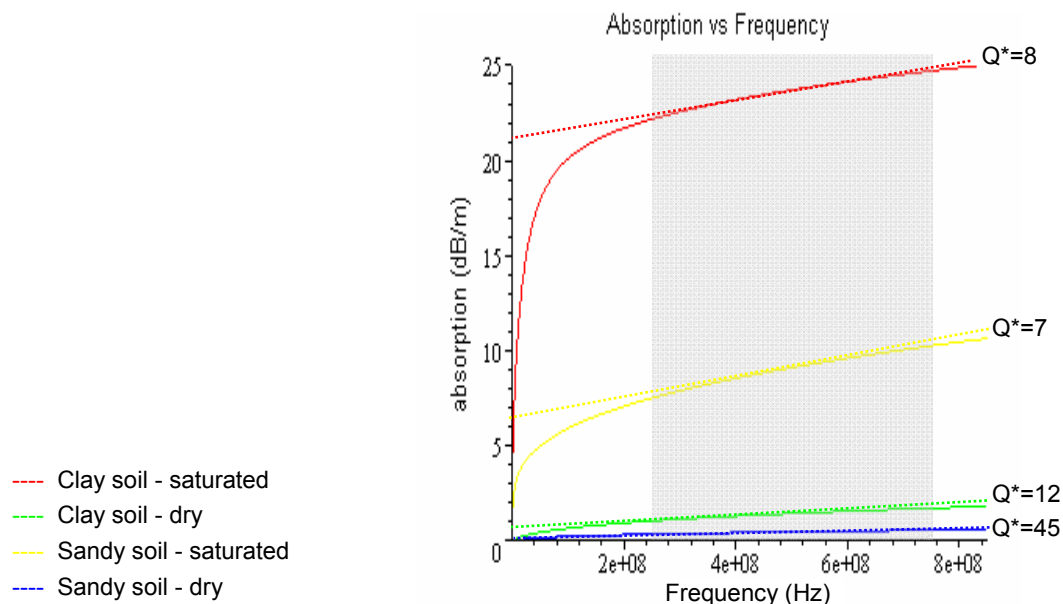

Figure 1: Absorption vs frequency for saturated clay soil, dry clay soil, saturated sandy soil and dry sandy soil. The dotted lines approximate the absorption vs frequency over the bandwidth of a 500 MHz GPR antenna (shown in grey).

The dotted lines in figure 1 show the approximation of the absorption vs frequency curves over the bandwidth of a 500 MHz antenna from which the Q*values were calculated. These lines do not pass through the origin and rarely do for geological materials. This means that, unlike seismic wave propagation GPR attenuation cannot be described by a constant Q. Q* however, can be used to describe the same change in wavelet shape as Q, although there is a difference in total amplitude.

As Q* is a function of conductivity, the variation of conductivity in the subsurface can be used to estimate how the attenuation of the GPR signal will vary. In other words, a conductivity (or resistivity) model can be used to determine a space and time varying inverse Q* filter. Q* can not be directly determined from DC resistivity values, since the effect of the imaginary part of the dielectric permittivity on the effective conductivity is not measured by an ERI survey. This is why the Q* values must be obtained from the GPR data through scanning, and a Q* model cannot be generated directly from the ERI inversion results The following example demonstrates how we have used ERI data to apply an inverse Q* filter to co-located GPR data.

Example - Archaeological site in Burgos, Spain

This data set was generously provided by WorleyParsons Komex. The Burgos site is known to be the location of a 16th to 19th century Christian church now buried beneath an open field and playground located near the Castillo in Burgos, Spain. During the construction of the playground in 1993, part of the site was excavated. Amongst the artefacts recovered were several Jewish artefacts. It is speculated that prior to being a Christian church, this was the site of a 15th century

Jewish synagogue that was either destroyed or modified to become the church. To identify archaeological excavation locations several geophysical surveys were acquired in July 2005. These surveys included a 3D GPR survey, a magnetic survey, and an ERI line.

The resistivity model (Figure 2) shows a highly resistive layer in the first two meters below ground surface with resistivities greater than 800 ohm-m (shown in yellow, orange and red). This was interpreted as the archaeological remains of the synagogue and/or church including building debris. The area of resistivity less than 200 ohm-m shown in shades of blue on the resistivity model was interpreted as the marl bedrock. This marl is conductive due to its high clay content.

The contact between the highly resistive layer and the bedrock (approximately the bright green on the resistivity model) represents the base of the structure's foundation that may have been cut into the bedrock. Where the bright green approaches the surface coincides with the location of a strong magnetic anomaly and was interpreted as a major structural wall.
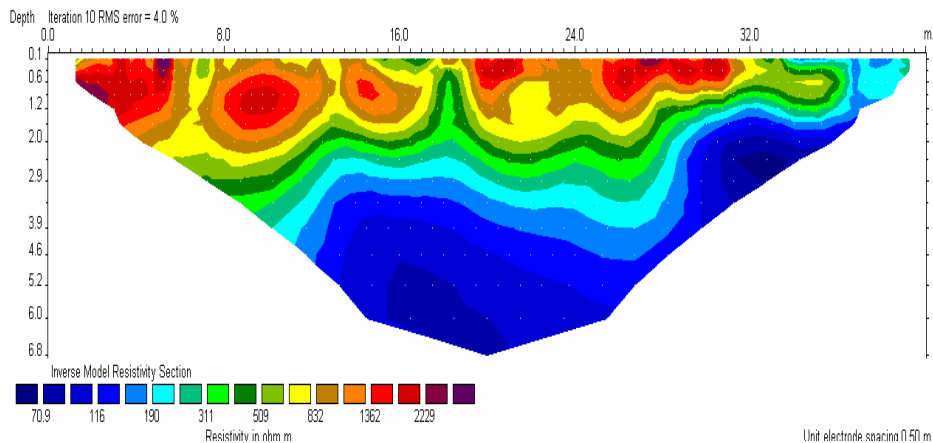

Figure 2: Inverted Resistivity model of the Burgos Spain line.

The GPR profile has a depth of investigation of 2 meters, barely resolving the bedrock. What was interpreted as a wall on the resistivity model appears on the GPR profile as a very shallow hyperbola. The archaeological remains appear as multiple diffractions on the right side of the profile.
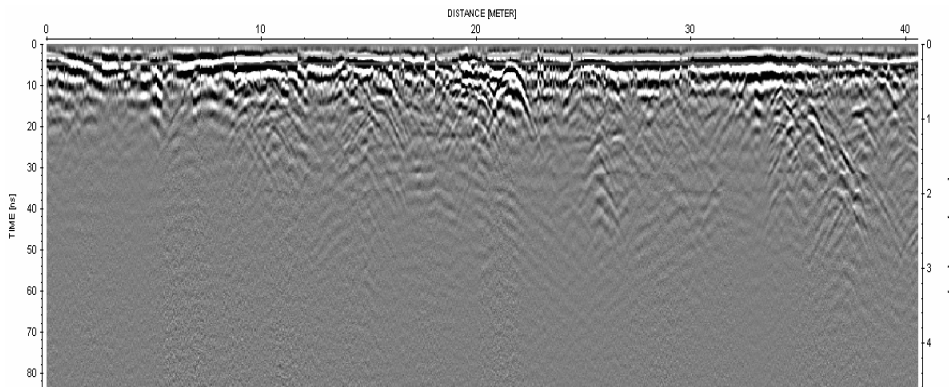

Figure 3: Input GPR line(opposite direction from ERI model).

Inverse Q* filtering with the time and space varying Q* model greatly improves the depth of investigation and the resolution of this GPR image as can be seen in Figure 4.
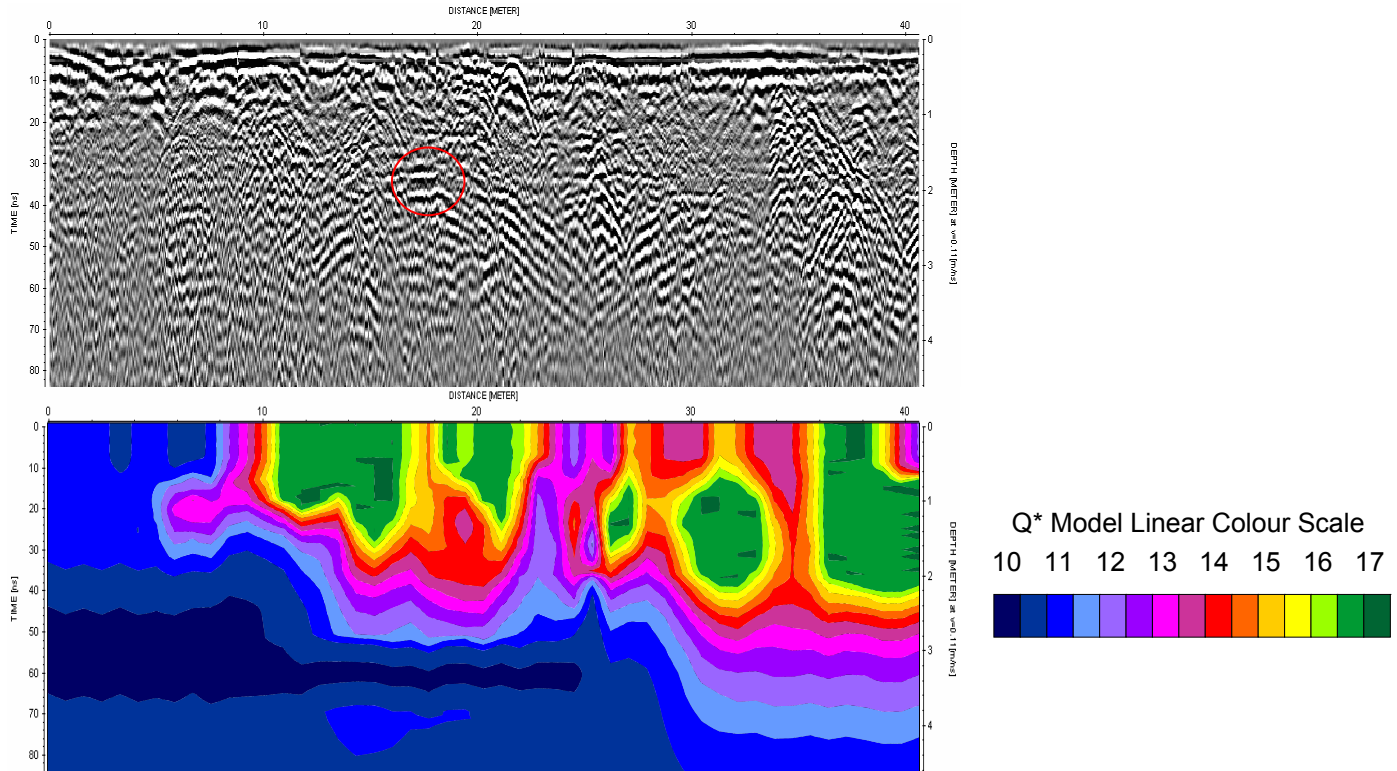

Figure 4:
Top - GPR profile from Burgos, Spain filtered with space and time varying Q* (10-17) model.
Bottom - Q* model from Burgos Spain

The top of bedrock is visible, particularly the mound-like structure in the centre of the image. The vertical resolution of the reflectors and diffractors above the bedrock is also improved. The enhanced amplitude balance of the diffractors on the right hand side of the image makes it easier to distinguish one from another and to see the flat reflectors that the diffraction tails cover. This is due to the high Q* values used at this location. One of these reflectors that is of importance to the interpretation, is that at 32 nanoseconds (approximately 1.8 meters deep). This reflector is fairly flat across the entire image and could definitely be the base of the structure foundation.

The time and space varying inverse Q* filter gives good separation of reflectors. An example of this is circled in red in Figure 4. This shows a strong flat reflection from the top of the mound like structure in the bedrock. Since this is also at about 1.8 meters deep, it supports the theory that this is the depth of the foundation base which has been cut into the bedrock at this location.

In this case the combination of the ERI and GPR surveys is successful in improving the vertical resolution of the image while maintaining reflector continuity, which has facilitated the interpretation of the base of the foundation and the cut bedrock. The amplitude balance in the filtered GPR profile also allows for precise separation and location of the archaeological remains.

Conclusions

With the rapid increase in the computing capacities of personal computer, the quantitative combination of near-surface geophysical surveys is an area where there are many new development opportunities. This work demonstrates a successful procedure for the combination of

GPR and ERI surveys. GPR attenuation is highly variable in the near-surface depending on the geology, in particular the clay content and the groundwater saturation and ion content. Since GPR attenuation is a function of conductivity, the inverted resistivity model from an ERI survey is used to apply a time and space varying attenuation or Q* correction to co-located GPR data. With this procedure, the Q* correction is optimized for the entire GPR profile resulting in an enhanced image with good amplitude balance, good separation of events and good vertical resolution. The lateral resolution is increased and the signal to noise ratio improved. One of the most striking aspects of the results is the increase in the depth of investigation of the GPR data.

Acknowledgements

References

Green, A. Lanz, E. and Maurer, H., 1999, A template for geophysical investigation of small landfills: *The Leading Edge*, February 1999, 248-255.

Irving, J.D. and Knight, R.J., 2003, Removal of wavelet dispersion from ground-penetrating radar data: *Geophysics*, 68 (3), 960-970.

Kjartansson. E., 1979, Constant Q wave propagation and attenuation: *Journal of Geophysical Research*, 84, 4737-4748.

Meju, Max., 2002, Environmental geophysics: Conceptual models, challenges and the way forward: *The Leading Edge*, May 2002, 460-464.

Olhoeft, G. R. and Capron, D. E., 1993, Laboratory Measurements of the Radio Frequency Electrical and Magnetic Properties of Soils from Yuma, Arizona: *U.S. Geological Survey Open-File Report*, 93-701.

Turner, G. and Siggins, A. F., 1994, Constant Q attenuation of subsurface radar pulses: *Geophysics,* 59 (8), 1192-1200.